Journal of Manufacturing Engineering, December 2014, Vol. 9, Issue. 4, pp 219-225

EFFECT OF HEAT INPUT ON MICROSTRUCTURE AND MECHANICAL PROPERTIES OF FRICTION STIR WELDED AA1100 ALUMINIUM JOINTS

Rajakumar S[1], Balasubramanian V[2]

[1]Assistant Professor, [2]Professor, Centre for Materials Joining and Research (CEMAJOR), Department of Manufacturing Engineering, Annamalai University

ABSTRACT

Friction stir welding process (FSW) is an emerging solid state joining process in which the material that is being welded does not melt and recast. The FSW process and tool parameters play a major role in deciding the joint characteristics. Therefore, mechanical properties should be controlled to obtain good welded joints. In this investigation, an attempt has been made to understand the effect of heat input on microstructure and mechanical properties of friction stir welded AA1100 aluminium joints. The joints are fabricated using different D/d ratio's (1.8, 2.4, 3, 3.6, and 4.2) and respect heat inputs (0.568, 0.758, 0.947, 1.137 and 1.326 kJ/mm). The joints fabricated with a D/d ratio of 3 (0.947kJ/mm) has yield superior mechanical properties.

Keywords: *Welding, Mechanical, Aluminium, Heat Input.*

1. Introduction

Friction stir welding (FSW) is a relatively new solid-state joining technique as illustrated in Fig.1. It has been extensively employed for aluminum alloys, as well as for magnesium, copper, titanium and steel. Compared to conventional fusion welding methods, the advantages of the FSW process include better mechanical properties, low residual stress and distortion, and reduced occurrence of defects [1-2]. This welding technique is being applied to the aerospace, automotive, and ship building industries, and it is attracting an increasing amount of research interest. FSW technology requires a thorough understanding of the process and the consequent evaluation of weld mechanical properties are needed in order to use the FSW process for production of components in aerospace applications. For this reason, detailed research and qualification work is required [3]. Based on friction heating at the faying surfaces of two sheets to be joined, in the FSW process a special tool with a properly designed rotating probe travels down the thickness of contacting metal plates, producing a highly plastically deformed zone through the associated stirring action. The localized thermo mechanical affected zone is produced by friction between the tool shoulder and the plate top surface, as well as plastic deformation of the material in contact with the tool [4]. The probe is typically slightly shorter than the thickness of the work piece and its diameter is typically slight larger than the thickness of the work piece [5]. The microstructure evolution and the resulting mechanical properties depend strongly on the variation of the processing parameters leading to a wide range of possible performances [6].

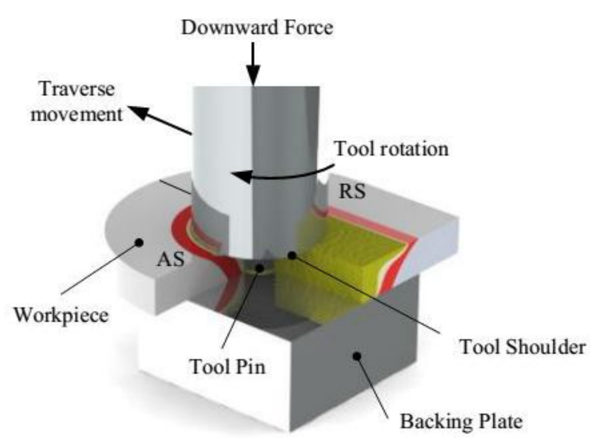

Fig. 1 – Friction Stir Welding Scheme.

2. Experimental Details

The base metals used in this investigation are AA1100 aluminium alloys. The chemical composition of the base metals was obtained using a vacuum spectrometer (ARL-Model: 3460). Sparks were ignited

**Corresponding Author - E- mail: ramanrachala@gmail.com*

at various locations of the base metal sample and their spectrum was analyzed for the estimation of alloying elements. The chemical composition of the base metals in weight percent is given in Table 1.Tensile and notched specimens were prepared as shown in Figs 2 & 3 to obtain the base metal tensile properties. ASTM E8M-05 guidelines were followed for preparing the test specimens.

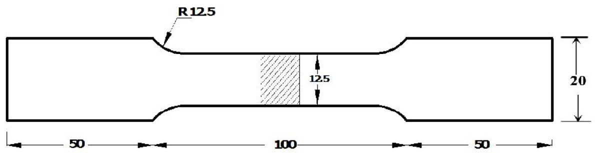

Fig 2. Dimensions of unnotched tensile test specimen (in 'mm')

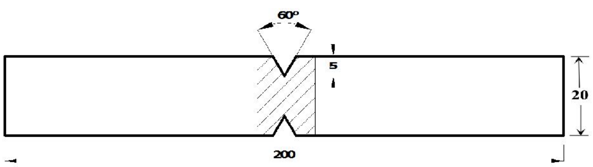

Fig 3. Dimensions of notched tensile test specimen (in 'mm')

Table 1: Chemical composition (wt. %) of base metals

Material	Mg	Mn	Fe	Si	Cu	Zn	Ti	Al
AA 1100	0.152	0.508	0.061	0.004	0.0015	0.0006	0.0016	Bal

Table 2: Mechanical properties of base metals

Material	Yield strength (MPa)	Ultimate tensile strength (MPa)	Elongation (%)	Vickers hardness at 0.05 kg load @ 15 Sec (HV)
AA 1100	105	110	32	70

Table 3: FSW process and tool parameters used to fabricated joints

Material	AA 1100
Welding Speed (mm/min)	100
Axial Force (KN)	0.508
Tool material	HCS
Shoulder diameter (mm)	9, 12, 15, 18, 21
Tool pin profile	Tapered pin
Pin diameter (mm)	5
Pin length (mm)	4.7
Tool inclination	0

Tensile test was carried out in 100 kN, servo controlled universal testing machine (Make: FIE – BLUESTAR, INDIA, Model: UNITEK 94100) with a cross head speed of 0.5 kN/min at room temperature. The 0.2% offset yield strength, ultimate tensile strength, and notch tensile strength were evaluated. The percentage of elongation was also evaluated and the values are presented in Table 2. Vickers's micro hardness testing machine (Make: Shimadzu and model: HMV-2T) was employed for measuring the hardness of the base metal with 0.05 kg load for 15 sec [ASTM E8 M-05a] and the values are recorded in Table 2. The microstructure of the as received base metals is shown in Fig. 4. Primarily the microstructure consists of elongated grains with uniform distribution of strengthening precipitates. The fractographs of tensile tested specimens (of base metals) are shown in Fig.5. The mode of fracture in all the specimens is ductile with micro-void coalescence.

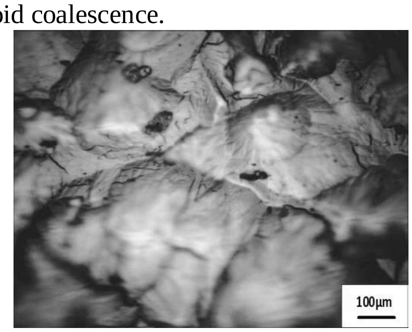

Fig. 4 Optical micrographs of base metals AA 1100

The rolled plates of 5 mm thickness, (the alloy, AA1100), were cut to the required size (300 x 150 x 5 mm) by power hacksaw cutting and milling. Square butt joint configuration was prepared to fabricate FSW joints.

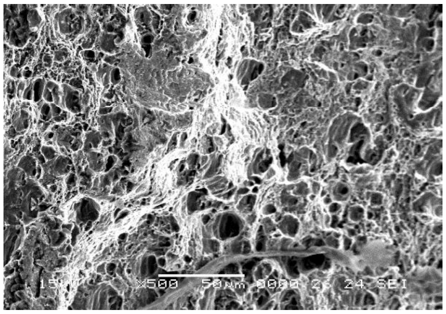

Fig. 5 Tensile fracture surface of base metals AA1100

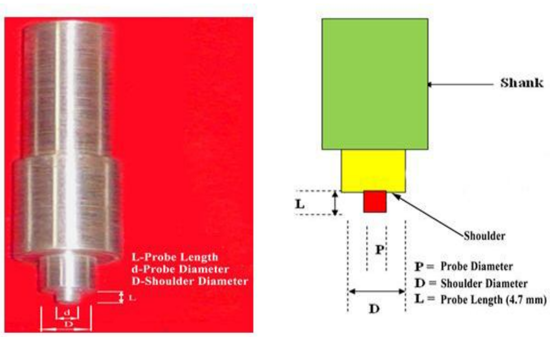

(a) Nomenclature of FSW tool

(b) Photographs of FSW tools

Fig. 6 Details of FSW tools

Fig. 7 Photographs of some of the fabricated FSW joints AA1100 Joints

The initial joint configuration was obtained by securing the plates in position using mechanical clamps. The direction of welding was normal to the rolling direction. Single pass welding procedure was used to fabricate the joints. Non-consumable tools made of high carbon steel were used to fabricate the joints. An indigenously designed and developed computer numerical controlled FSW (22 kW; 4000 RPM; 60 kN) was used to fabricate the joints. Photographs of FSW machine and close up view are displayed in Fig. 6(a) & (b). The tool nomenclature is shown in Fig.6 (a). The photographs of the tools are displayed in Fig. 6 (b). The details regarding tool dimensions and welding parameters used to fabricate the joints are presented in Table 3. The photographs of some of the fabricated joints are displayed in Fig. 7. The welding parameters and tool details are presented in Tables 3. Heat input was calculated using the following equation proposed by Heurtier et al. [6].

$$Q = \pi/3S \text{ x } \mu \text{ x } P \text{ x } \omega \text{ x } R_s \text{ x } \eta \quad (1)$$

The specimens for metallographic examination were sectioned to the required sizes from the joint comprising FSP zone, TMAZ, HAZ and base metal regions and then polished using different grades of emery papers. Final polishing was done using the diamond compound (1µm particle size) in the disc polishing machine. The polished samples were etched using 10% NaOH to show general flow structure of the alloy. A standard Keller's reagent made of 5 ml HNO_3(95% concentration), 2 ml HF, 3ml HCL, 190 ml H_2O was used to reveal the microstructure of the welded joints. Macro and micro-structural analysis have been carried out using a light optical microscope (VERSAMET-3) incorporated with an image analyzing software (Clemex-Vision). The fractured surfaces of the tensile tested specimens were examined by a Scanning Electron Microscope (SEM) to reveal the fracture surface morphology.

3. Results and Discussion

3.1 Effect of the heat input on the Macrostructure

Top surface of the welded joints (beads) are free from visible in Fig. 7. However, the weld cross section at low magnification shows defects such as tunnel defect and worm hole. From the Table 4 clearly shows that Heat input is low or high defect will occur. In the heat input of 9.47 kJ/mm yielded defect free joints compared with other heat inputs. The effect of tool shoulder diameter on macrostructure of the weld cross section was illustrated in Table.4 Of the five joints fabricated, the joint fabricated using a tool with shoulder diameter of 15 mm (3 times the plate thickness) and heat input of 0.947KJ/mm yielded better tensile properties.

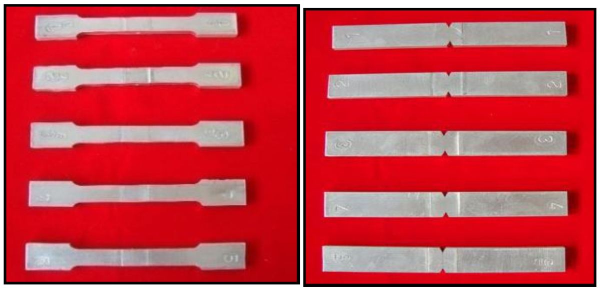

(a) AA1100 Aluminium

Fig 9. Photographs of unnotched and notched tensile specimens (Before testing)

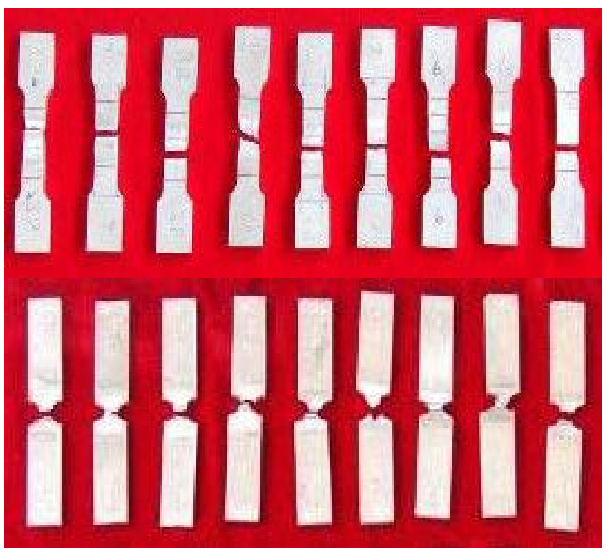

(b) AA1100 Aluminium

Fig 10. Photographs of unnotched and notched tensile specimens (After testing)

3.2 Effect of the heat input on the Microstructure

In this investigation an attempt was made to understand the effect of heat input and its subsequent influence on microstructure, microhardness and tensile strength of friction stir welded joints of AA1100 alloy, Table. 4 shows the effect of D/d ratio on tensile strength of FSW joints of AA 1100 alloy, Table. 4 presents the effect of tool shoulder diameter on macrostructure, microstructure of FSW joints of AA 1100 aluminium alloy. In the shoulder influenced region between the Al alloy base material and the stir zone. The grain size can be clearly seen to decrease as it transitions from the base material.

It should be observed that elongated grains were observed even in the parent material with particular reference to the central zone of the joint section Table.4 shows the optical micrographs of weld nugget of all the joints. It is due to the stirring action at plastic condition of the metal during FSW. This phenomenon was also reported by other investigators [8-9]. Table 4 in the heat input low at 5.68 kJ/mm in D/d ratio of 1.8 coarse and elongated grain are formed due to low heat input and diameter of grain is 63µm. Table 4 in the heat input high at 1.326 kJ/mm in D/d ratio of 4.2 produce fine grains are formed and same time in these condition high heat input will produced the worm hole defect at bottom of weld nugget region. Regardless of welding condition, Table 4 in the heat input at 0.947 kJ/mm in D/d ratio of 3 fine grains are formed due these fine grains produced more strength and defect free from the weld region.

3.3 Effect of the heat input on the Surface morphology

Table 4 clearly shows that Heat input is low or high defect will occur. While the heat input and shoulder diameters increases with the grain sizes is decreases due to insufficient or inadequate heat input. Heat input varies from 0.568 to 1.326kJ/mm its shows in Table 4. In table.4 shows low heat input and small D/d ratio of surface produce the defect of worm hole and coarse and elongated dimples will formed. And table4 shows high heat input and large D/d ratio of surface produce the defect of worm hole and fine dimples formed in along the weld direction and table.4 Shows optimum heat input and 3 D/d ratio formed fine dimples, more strength and defect free zone. Regardless of welding condition, severe particle coarsening and clustering were observed in the vicinity of the tensile fractured area of FSW specimens. The Table 4, shows the SEM fractographs of all the specimens. It was noted that the tensile fracture mode was significantly altered with varying welding parameters in the friction stir welded Al 1100 joints.

3.3 Effect of the heat input on the Mechanical Properties

3.3.1 Tensile properties

The dimension of tensile specimen is presented in Fig. 2. The specimen before and after tensile testing are displayed in Table.4. In each condition, specimens were tested and the average of results is presented in table.4 shows of the joints, the joint fabricated using a tool with shoulder diameter of 15 mm (3 times the plate thickness) of heat input 0.947kJ/mm yielded better tensile properties.

3.3.2 Hardness

In welded joints, the failure will occur along the weakest region (lowest hardness region). Normally, the hardness profile was measured either along the mid thickness of welded plate or along the top, center and bottom of the plate thickness to determine the lowest hardness points [7,8,9]. However it should be pointed out that such hardness profiles could not predict the fracture behavior of welded joints because of limited hardness points. In this study, the hardness distribution profile graphs were constructed by measuring the Vickers micro-hardness at an interval of 1 mm along the cross section of FSW joint.

Colligan [10] investigated the material flow behavior of FSW aluminum alloy. During FSW mainly, the two effects are responsible for the creation of the material flow in the stir zone. First is the extrusion process, where the applied forces and the motion of the tool pin propel the material after it has undergone the plastic deformation. The second is due to the rotation of the pin that serves as the driving force for the flow. Due to high values of viscosity, the stirring effect is much more distinct in comparison to the extrusion driven flow. Since FSW is a hot working process, the temperature required for welding must reach well above the recrystallization temperature of the materials to be joined so as to derive the benefits of dynamic recrystallization in the stir zone. The material will attain the required temperature only when the welding conditions and the parameters are selected properly during FSW [11]. Under these circumstances, tool shoulder diameter plays a vital role since it is considered to be the primary source of heat generation. It can also be understood from Eq. (1), the tool shoulder radius is having directly proportional relationship with the frictional heat generation.

From Table 4, the following inferences can be obtained:

i. The larger tool shoulder diameter (21 mm) lead to wider contact area and resulted in inadequate heat input along the weld and subsequently the tensile strength (72MPa) of the joints are riorated.

ii. The smaller tool shoulder diameter (9 mm) lead to narrow contact area and resulted in less frictional heat generation and hence the weld metal consolidation is not good in the FSP region and subsequently resulted in lowest tensile strength(56MPa).

iii. Of the five joints fabricated using different tool shoulder diameters, the joint fabricated using the tool with 15 mm shoulder diameter exhibited superior tensile strength (81MPa) and heat input is 9.47KJ/mm (Table 4).

iv. Due to this 15mm shoulder diameter yielded high hardness, high tensile properties and smaller grains (22.5μm).

In this investigation, joints were fabricated using five tools. Of the joints, the joint fabricated using a tool with the shoulder diameter of 15 mm (3 times plate thickness) of heat input 0.947kJ/mm yielded higher tensile strength and this is mainly due to the formation of defect free stir zone. The joints fabricated by all other tools yielded lower tensile strength due to the presence of defect in stir zone and it is evident from macro structure analysis (Table 4). In all the joints, macro level defects are not visible in shoulder influenced region and shoulder-pin influenced region. But the pin influenced region, especially the swirl zone, contains some form of defects. The joint fabricated by a tool with shoulder diameter of 9 mm of heat input 0.568kJ/mm, contains a huge tunnel defect in the advancing side of pin influenced region. Similarly, the joint fabricated by a tool with shoulder diameter of 12 mm also contains a worm hole at the same location. The joint fabricated by a tool with the shoulder diameter of 18 & 21 mm and heat input 1.137 & 1.326kJ/mm also contains a tunnel defect at the same location but much larger in size. This suggest that increasing the tool shoulder diameter from 9 mm and heat input 0.568kJ/mm reduces the size of the defect at swirl zone and tool shoulder diameter of 15 mm and heat input 0.948kJ/mm completely eliminated the formation of defect at swirl zone.

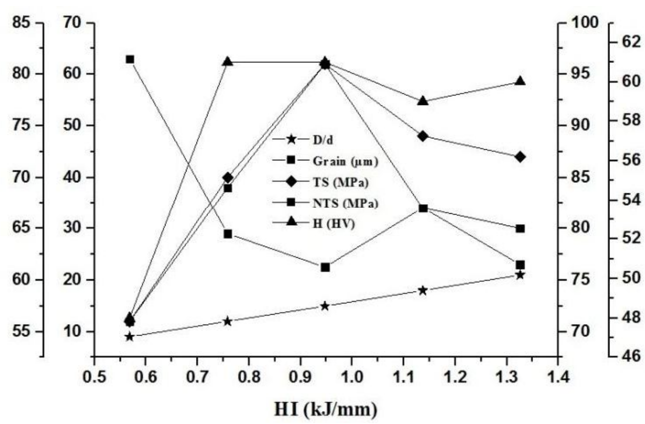

Fig.11 Effect of Heat Input on D/d ratio, Tensile properties, Hardness and grain sizes.

Table 4. Effect of tool shoulder diameter on macrostructure and microstructure in AA1100 aluminium alloy.

D_S	D/d	H.I	Strength Properties		Macro graph of joint cross-section	Micrograph of FSP region	Factograph of fracture surface	Observations
9	1.8	5.68	T.S	56	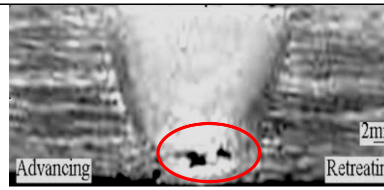	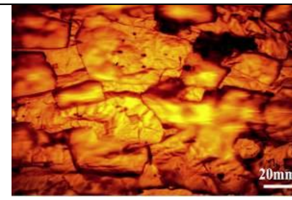	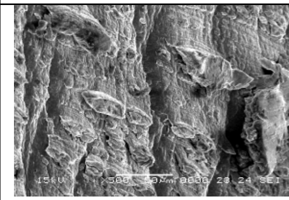	(i) Name of the defect: Worm hole (ii)Location of the defect: Weld nugget (iii)Reason for the defect: Insufficient heat input (iv)Location of failure: along the weld (v)Average grain diameter: 63µm (vi)Fracture morphology: Coarse and elongated dimples
			N.T.S	71				
			H	48				
12	2.4	7.58	T.S	70	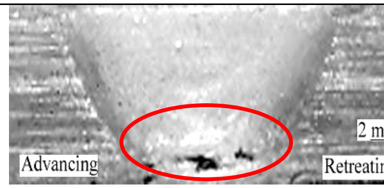	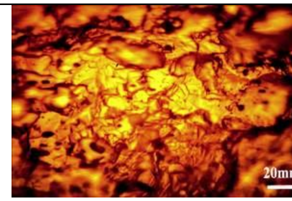	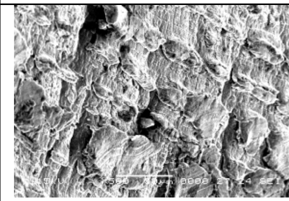	(i)Name of the defect: Worm hole (ii)Location of the defect: Advancing side (iii)Reason for the defect: lower heat input (iv)Location of failure: Weld nugget (v)Average grain diameter: 29µm (vi)Fracture morphology: Quasi-cleavage
			N.T.S	84				
			H	61				
15	3	9.47	T.S	81		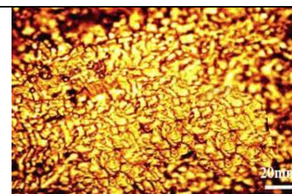	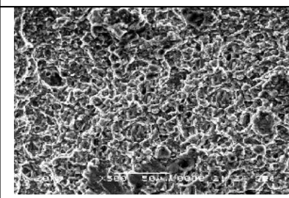	(i)Name of the defect: Defect free (ii)Location of the defect: Nil (iii)Reason for the defect: Adequate heat input (iv)Location of failure: Along the weld (v)Average grain diameter: 22.5 µm (vi) Fracture morphology: Fine dimples
			N.T.S	96				
			H	61				
18	3.6	11.37	T.S	74		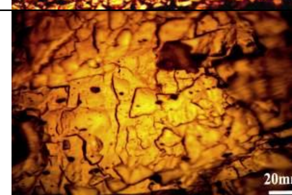	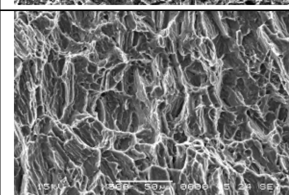	(i)Name of the defect: Tunnel (ii)Location of the defect: Retreating side (iii)Reason for the defect: Inadequate heat input (iv)Location of failure: TMAZ (v)Average grain diameter: 34µm (vi)Fracture morphology: Coarse dimples
			N.T.S	82				
			H	59				
21	4.2	13.26	T.S	72	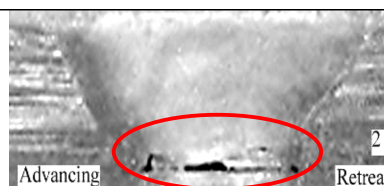	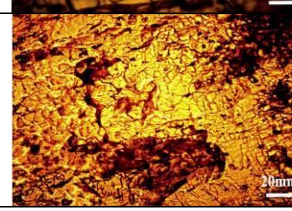	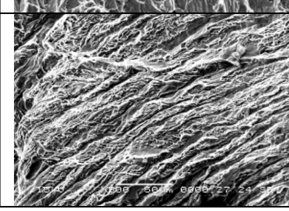	(i)Name of the defect: Worm hole (ii)Location of the defect: Weld nugget (iii)Reason for the defect: Inadequate heat input (iv)Location of failure: Along the weld (v)Average grain diameter: 23µm (vi)Fracture morphology: Fine dimples
			N.T.S	80				
			H	60				

i. T.S-Tensile Strength (MPa); N.T.S - Notch Tensile Strength (MPa); H- Hardness (HV); D_S- Shoulder Diameter (mm);
ii. H.I- Heat Input (KJ/mm)

4. Conclusions

In this investigation, the tensile properties of similar aluminum (AA 1100) joints were evaluated. Of the joints fabricated using tools with different shoulder diameters, the joint fabricated with a tool shoulder diameter of 15 mm (3 times the plate thickness) yielded maximum tensile strength of 81 MPa the joint efficiency is 77.14% compared with the lower strength base metal and notch tensile strength of 96 Mpa.

References

1. *Thomas W M (1991), "Friction Stir Welding" International Patent Application No. PCT/GB92/02203 and GB Patent Application No. 9125978.8. U.S. Patent No 5, 460; 317.*

2. *Dawes C J (1995), "An Introduction to Friction Stir Welding and its Development" Weld Metal Fabric Vol.63, 2–16.*

3. *Thomas W M and Nicholas E D (1997), "Friction Stir Welding for the Transportation Industries" Mater and Des, Vol. 18, 269–273.*

4. *Oosterkamp A, Djapic Oosterkamp L, and Nordeide A (2004), "Kissing Bond Phenomena in Solid State Welds of Aluminum Alloys", Weld Journal, 225–31.*

5. *Zeng W M, Wu H L and Zhang J (2006), "Effect of Tool Wear on Microstructure Mechanical Properties and Acoustic Emission of Friction Stir Welded 6061 Al Alloys", Acta Metall Sinica, Vol. 19(1), 9–19.*

6. *Song L, Hu Y, Wang S, Chen Z and Fan W (2002), "Study on the Solvothermal Preparation of Polyenthylene/Organphilic Monymorillonite Nanocomposites", Journal of Materials Chemistry, Vol. 12 (2), 3152-3155.*

7. *Heurtier P, Jones M J, Desrayaud C, Driver J H, Montheillet F and Allehaux D (2006), "Mechanical and thermal modelling of friction stir welding", J Mater Process Technol, Vol.171, 348–57.*

8. *Barcellona A, Buffa G, Fratini L amd Palmeri D (2006), "On microstructural phenomena occurring in friction stir welding of aluminium alloys", J Mater Process Technol, Vol. 177, 340–3.*

9. *Lim Sunggon, Kim Sangshik, Lee Chang-Gil and Kim Sungjoon (2004), "Tensile behavior of friction-stir-welded Al 6061-T651", Metall Mater Trans A;35:2829–35.*

10. *Mishra R S and Ma Z Y (2005), "Friction stirr welding and processing", Mater Sci Eng [A]50:1–78.*

11. *Colligan K (1999), "Material flow behaviour during friction stir welding of aluminium" Weld J, 229–37.*

12. *Oosterkamp A, Djapic Oosterkamp L and Nordeide A (2004), "Kissing bond phenomena in solid state welds of aluminum alloys", Weld J, 225–31.*

